Glial cells influence tubulin polyglutamylation patterns in neurons

Jeffrey Paer
Neurobiology Report – Final Revision
Bio324/Neurobiology
Wheaton College, Norton, Massachusetts, USA
November 12, 2014

Introduction

Microtubules serve critical roles in neuronal morphogenesis (Sakakibara et al. 2013). At an early stage in neuronal development, microtubules function as an inner scaffolding for the growth of neurites, or cytoplasmic processes protruding from the neuron that eventually become axons and dendrites (Sanchez et al. 2000). The dynamic activity of microtubule shortening and elongation underlies the neurite retraction and extension characteristic of neuronal differentiation, and is contingent upon microtubule stability (Sakakibara et al. 2013). Microtubules also function as physical pathways for the transport of organelles and protein-carrying vesicles between neuronal cell bodies and neurite terminals required for proper neuronal development (Sanchez et al. 2000).

Tubulin, or the monomeric constituent of microtubules, can undergo a variety of post-translational modifications that modulate microtubule stability and function (Kandel et al. 2000). One such modification that is particularly significant to neuronal differentiation is the polyglutamylation of the C-termini of α- and β-tubulin subunits (Ikegami et al. 2006). Since many microtubule-associated compounds bind to tubulin C-termini, tubulin polyglutamylation is proposed to function as a molecular marking system that regulates the activity of microtubule-associated proteins (MAPs), molecular motors, and microtubule-severing proteins (O'Hagan and Barr 2012). For example, the affinity of MAPs to microtubules is correlated with the length of glutamyl side chains (Wloga and Gaertig 2011). Generally speaking, the longer the glutamyl side chain, the greater the likelihood of MAP-tubulin binding, and the higher the degree of MAPs' stabilizing effects on microtubule dynamics (Sonia et al. 2012).

In regulating the binding affinity of microtubule-stabilizing MAPs, tubulin polyglutamylation is suggested to play a role in neurite development and maintenance (Wloga and Gaertig 2011). While the levels of α-tubulin polyglutamylation are relatively constant throughout neuronal development, the levels of polyglutamylated β-tubulin progressively increase, suggesting that the glutamylation of the β-subunit may be necessary for neuronal development (Audebert et al. 1994). A recent study showed that the knockdown of TTLL7 mammalian β-tubulin polyglutamylase mRNA resulted in the inhibition of neurite outgrowth *in vitro*, suggesting that polyglutamylated β-tubulin is required for the growth of neurites (Ikegami et al. 2006). While polyglutamylated microtubules perform a range of functions in regulating microtubule-associated components and ultimately neuronal differentiation, it is possible that tubulin polyglutamylation is essential for the recruitment and activity of MAPs in facilitating microtubule dynamics (Sakakibara et al. 2013; O'Hagan and Barr 2012; Wloga and Gaertig 2011).

The regulation of tubulin glutamylation is an intriguing area of research because it is suggested to be a molecular process involved in neurodegeneration and regeneration (O'Hagan and Barr 2012). Neuron damage has been shown to induce the expression of tubulin deglutamylases in both rodents (Harris et al. 2000) and *C. elegans* (Chen et al. 2011). It has also been postulated that the interactions between polyglutamylated β-tubulins and tau, a MAP associated with Alzheimer disease, correlate with dendritic neurite growth (Ikegami et al. 2006). In addition to neuronal tubulin polyglutamylation patterns and MAP function, glial cells have been shown to influence neuronal development through the local release of growth factors, such as the neurotrophic growth factor (NGF) (Kandel et al. 2000). Therefore, studying the relationship between glial cells and tubulin polyglutamylation patterns in neurons may contribute to understanding the roles of tubulin polyglutamylation in neurodegenerative disorders.

Considering the function of glial cells in releasing trophic factors that promote neuronal cell growth (Kandel et al. 2000), and that neurite development may necessitate the polyglutamylation of β-tubulin (Audebert et al. 1994), it was hypothesized that glial cells influence tubulin glutamylation patterns in neurons. The present study used *Gallus gallus* as a model due to the precedence of the organism's use in nervous system tissue culture (Morris and Hollenbeck 1993), and performed immunofluorescent labeling to test the two-pronged hypothesis: (1) that proximal neuronal regions in contact with glial cells have a greater polyglutamylated tubulin profile than distal neuronal regions, and (2) that neuronal regions near a neighboring but non-contacting glial cell will have a greater polyglutamylated tubulin

profile than neuronal regions positioned further away.

Materials and Methods

Materials

Dr. Robert Morris supplied sea urchin plutei larvae (*Lytechinus pictus*) collected on July 13, 2014 to be used as positive controls for immunofluorescent staining. All nervous system tissue culture media and supplements, and the mouse FITC-conjugated anti-alpha-tubulin (DM1A) and mouse anti-polyglutamylated-tubulin antibodies were acquired from Sigma-Aldrich Co. (St. Louis, MO). Alexafluor 546-conjugated goat anti-mouse IgG and Hoechst DNA stain was acquired from Molecular Probes, Inc. (Eugene, OR). Imaging was conducted in the Imaging Center for Undergraduate Collaboration (ICUC) at Wheaton College (Norton, MA) at the Zodiac and Capricorn workstations. The Zodiac workstation consisted of a Nikon Eclipse E801 Epi-Fluorescence Microscope, 0.76X camera mount and SPOT RT3 camera from Diagnostic Instruments, Inc. (Sterling Heights, MI), and SPOT Software (version 4.6) on an iMAC desktop computer (Mac OSX version 10.5.8). The Capricorn workstation consisted of a Nikon Eclipse E400 Microscope, 1.0X camera mount and SPOT Insight 2 camera from Diagnostic Instruments, Inc. (Sterling Heights, MI), and SPOT Software (version 4.6) on an iMAC desktop computer (Mac OSX version 10.5.8).

Cell Culture

Sympathetic nerve chain and dorsal root ganglia were dissected from 10-day old chick embryos (*G. gallus*) and cultured as whole ganglia or dissociated neurons and glia plated on coverslips as previously described (Morris and Hollenbeck 1993; Morris, “Primary culture of chick embryonic peripheral neurons1: dissection” 2014). Note that the drop of laminin applied to the coverslips was at a 1:500 dilution. Six total coverslips topped with chick embryonic nervous system tissue were then incubated in F-plus medium (Leibovitz L-15, 2 mM L-glutamine, 0.6% glucose, 10% fetal bovine serum, 100 U, ug/mL penicillin, streptomycin, and 50 ng/mL NGF) at 37°C for a week prior to fixation.

Nervous System Tissue Fixation, Permeabilization, Rehydration, and Blocking

After a week of incubation at 37°C, half of the nervous system tissue cultures were fixed with formaldehyde/glutaraldehyde and permeabilized with a fix/perm buffer, and the other half was fixed and permeabilized with methanol as previously described (Morris, “Immunofluorescence of chick neuronal primary cultures” 2014). Two coverslips coated with sea urchin plutei larvae (*L. pictus*) were also fixed with formaldehyde and glutaraldehyde and permeabilized with the fix/perm buffer, and were used as positive controls in the immunofluorescent labeling (Morris, “Immunofluorescence of chick neuronal primary cultures” 2014).

The methanol-fixed and permeabilized chick embryos were then rehydrated with a phosphate-buffered saline and Triton X-100 (PBS-T) solution as previously described (Morris, “Immunofluorescence of chick neuronal primary cultures” 2014). Next, all of the fixed and permeabilized chick embryos and sea urchin plutei larvae were blocked with a PBS-T solution containing 3% Bovine Serum Albumin (BSA) by submerging the coverslips in approximately 2 mL of block buffer in a six-well plate.

Immunofluorescent Labeling of Fixed Embryos

The antibody labeling of the fixed, permeabilized and blocked chick embryonic and sea urchin larvae tissue was conducted as previously outlined (Morris 2013). In addition to the Hoechst DNA stain, three antibodies were used in this study: mouse FITC-conjugated anti-alpha-tubulin (DM1A), mouse anti-polyglutamylated-tubulin, and Alexafluor 546-conjugated goat anti-mouse IgG. Each antibody treatment consisted of 200 uL antibody applications. Different antibody concentrations and incubation conditions were applied to each cell-coated coverslip. All antibody-treated samples were incubated in humidity chambers constructed from a large petri dish covered with a layer of Parafilm that was studded with Eppendorf tube caps (to serve as platforms to support coverslips). Several Kimwipes saturated with autoclaved water were placed around the perimeter of the bottom of the petri dish and plastered to the dish’s cover. The humidity chamber was covered with aluminum foil during incubations to prevent photobleaching. Following all incubation periods, the coverslips were washed with approximately 3 mL of PBS-T three times at five minutes per wash. The coverslips were then submerged in block buffer and stored in 4°C under aluminum foil before the Hoechst DNA stain treatment, coverslip mounting, and imaging.

The negative control consisted of one formaldehyde/glutaraldehyde-treated chick sample treated with Alexafluor 546-conjugated goat anti-mouse IgG (1:200 dilution) and incubated overnight at 4°C. The negative control functioned to determine if auto-fluorescence of the antibodies would occur through non-specific binding of the Alexafluor 546-conjugated goat anti-mouse IgG. Note that no methanol-fixed negative controls were prepared because another lab member accidentally took the negative controls (intended to be used in this experiment) for their own experiments.

The positive controls consisted of two formaldehyde/glutaraldehyde -treated sea urchin plutei larvae samples

treated with mouse anti-polyglutamylated-tubulin (1:1000 dilution), Alexafluor 546-conjugated goat anti-mouse IgG (1:200 dilution), and mouse FITC-conjugated anti-alpha-tubulin (DM1A) (1:100 dilution). Each antibody treatment was followed by an hour-long incubation period at room temperature (22-25°C). The positive controls functioned to determine the effectiveness of the antibody treatments, as the mouse anti-polyglutamylated-tubulin and mouse FITC-conjugated anti-alpha-tubulin antibodies have been reported to successfully react in *L. pictus* (according to their manufacturers).

Five fixed and permeabilized chick embryonic nervous system tissue samples served as experimental groups. One methanol-fixed chick sample and one formaldehyde and glutaraldehyde-fixed chick sample were treated with mouse anti-polyglutamylated-tubulin (1:1000 dilution), Alexafluor 546-conjugated goat anti-mouse IgG (1:200 dilution), and mouse FITC-conjugated anti-alpha-tubulin (DM1A) (1:100 dilution), and subjected to one-hour incubations at room temperature. The second methanol-fixed chick sample was treated with the same concentrations of antibodies, but subjected to overnight incubations at 4°C. The third methanol-fixed chick sample and second formaldehyde/glutaraldehyde-fixed chick sample were treated with mouse anti-polyglutamylated-tubulin (1:500 dilution), Alexafluor 546-conjugated goat anti-mouse IgG (1:100 dilution), and mouse FITC-conjugated anti-alpha-tubulin (DM1A) (1:100 dilution), and subjected to one-hour incubations at room temperature.

Just prior to mounting and imaging the coverslips, each sample was subjected to a 5 minute Hoechst DNA stain treatment. More specifically, each coverslip was washed with 2 mL of the Hoechst buffer (1:10,000 dilution in DMSO) for 5 minutes, washed 3 times with PBS-T as previously described, and submerged in block buffer until mounting.

Mounting and Imaging

The antibody and Hoechst DNA stain-treated samples were mounted onto microscope slides using nail polish as a sealant as previously described (Morris 2013). A droplet of block buffer was placed on each of the microscope slides. One of the positive control coverslips was mounted on top of coverslip chips, while the rest of the antibody-treated samples were placed cell-side down directly onto the block-buffer droplet-covered microscope slides.

The slides were then imaged at 40X objective magnification using either the Zodiac or Capricorn workstations in Wheaton College's ICUC (see Materials section). Imaging protocols were followed according to the workstation-specific protocols supplied by the ICUC. Note that the exposure times used in the imaging ranged from 550 milliseconds to a maximum of 10 seconds. Four total images were taken per slide location, including a phase contrast and blue, green and red fluorescent channels. Multiple slide locations were imaged per slide.

Quantification of Polyglutamylated-Tubulin Profiles

Polyglutamylated-tubulin profiles were expressed as the ratios of the mean polyglutamylated-tubulin signals to the mean α-tubulin signals corresponding to equally sized areas at particular neuronal regions. The mean signals from each antigen-corresponding fluorochrome were determined using the program ImageJ. More specifically, images of the green and red fluorescence channels (corresponding to the visualization of the α-tubulin and polyglutamylated-tubulin antigens respectively) from a given slide location were opened in Image J. A neuronal region of interest was selected on the image of the α-tubulin signal, and its "total mean brightness" was calculated using the "Analyze → Measure" function. To account for fluorescent noise, the same selected region was then moved to an area of background nearby (not containing any bright fluorescent signal) and its mean brightness was calculated. This value was the "mean noise." The true mean signal of α-tubulin at the neuronal region of interest was calculated by subtracting the "total mean brightness" by the "mean noise." The same process was then done for the image of the polyglutamylated-tubulin signal at the corresponding neuronal region of interest. Mean brightness values (of arbitrary brightness units on ImageJ) for both α-tubulin and polyglutamylated tubulin at neuronal regions of interest were recorded for each experimental slide. 18 data sets were collected from multiple neuron and contacting-glial cell interactions, and 7 data sets were collected from multiple neuron and neighboring but non-contacting (NBNC) glial cell interactions.

To test the hypothesis that proximal neuronal regions in contact with glial cells have greater polyglutamylated tubulin profiles than distal neuronal regions, parameters describing proximal and distal neuronal regions were established. Proximal neuronal regions were defined as areas within 5 microns of the edge of a contacting glial cell, while distal neuronal regions were defined as areas more than 20 microns away from the edge of the contacting glial cell. When testing the hypothesis that neuronal regions proximal to NBNC glial cells have a greater polyglutamylated tubulin profile than distal neuronal regions, proximal neuronal regions were defined as areas within 40 microns of the edge of the NBNC glial cell and distal neuronal regions were defined as areas more than 100 microns away from the edge of the NBNC glial cell. Length was determined by using the line-drawing function on ImageJ to measure the distance from a neuronal region of interest to the glial cell of interest.

The parameter of length was quantified by manually setting a pixel to micron scale for images produced at both the Zodiac and Capricorn workstations (see Materials section). Micrometer images specifically produced by the Zodiac

and Capricorn workstations were opened on ImageJ, lines were drawn from the micrometers' zero marks to the 100 micron marks, and the lines' corresponding pixel lengths were equated with 100 microns. The scales for the images produced at the Zodiac and Capricorn workstations were 4.190 pixels/micron and 5.330 pixels/micron respectively.

The unit-less brightness values for α-tubulin and polyglutamylated tubulin at neuronal regions proximal and distal to contacting and NBNC glial cells were averaged and the data sets' standard deviations were determined using Microsoft Excel. Polyglutamylated-tubulin profiles for each parameter were calculated by determining the ratio of the averaged polyglutamylated tubulin brightness values to the averaged α-tubulin brightness values.

Statistical Analyses

One-tailed two-sample Student's t-tests were used (on Microsoft Excel) to determine if the polyglutamylated-tubulin to α-tubulin mean signal ratios at proximal and distal neuronal regions were statistically different from one another.

Results

To test the hypothesis that glial cells influence tubulin polyglutamylation patterns in neurons, chick embryonic nervous system tissue was stained with a series of immunofluorescent antibodies to observe the α-tubulin and polyglutamylated tubulin antigens. Figure 1 depicts an image of a neuron and several glial cells used to quantify the polyglutamylated tubulin profiles of neuronal regions associated with both contacting and NBNC glial cells. Note that no blue, green or red fluorescence were visualized in the negative control slide (no Hoechst DNA stain or antibodies were applied to the negative control coverslip) suggesting that the fluorescence observed in the image (Fig. 1) was due to fluorescently labeled DNA, α-tubulin, and polyglutamylated tubulin. These data are not included. The positive control emitted light when illuminated in each fluorescent channel at the exposure times used, indicating the efficacy of the antibodies used and their reactivity in *L. pictus* (Fig. 2).

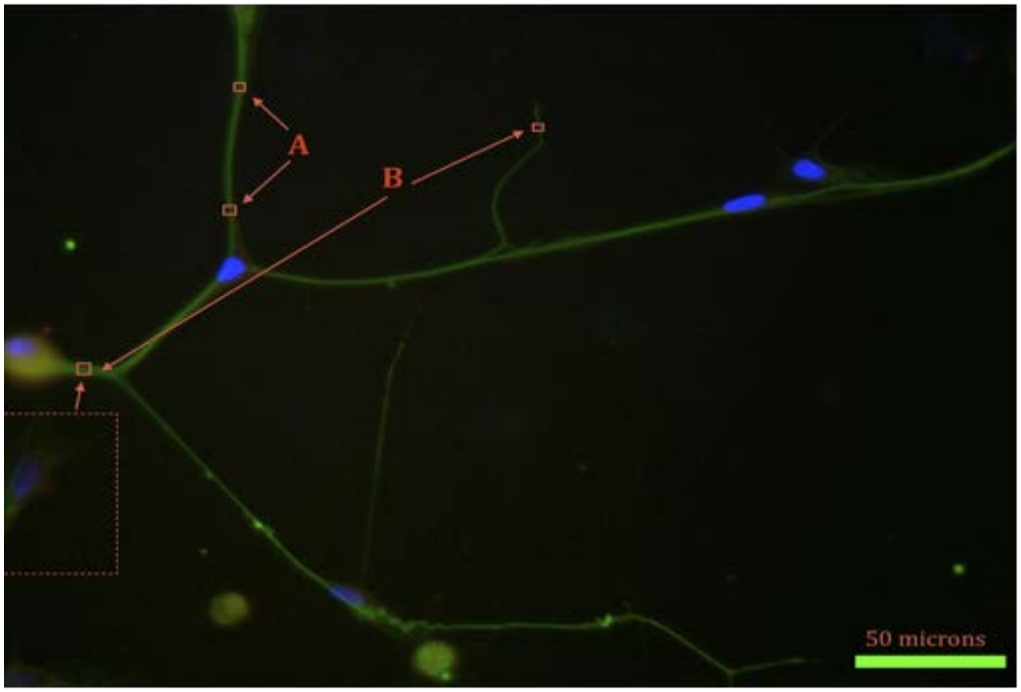

Fig. 1. Sympathetic neuron fixed with methanol, and stained with Hoechst (blue; DNA), FITC-DM1A (green; α-tubulin), and anti-polyglutamylated tubulin (red; polyglutamylated tubulin), and imaged at 40X objective magnification with a Nikon Eclipse E801 Epi-Fluorescence Microscope. (A) represents an example of glial cell-contacted proximal and distal neuronal regions analyzed, while (B) represents an example of glial cell-neighbored proximal and distal neuronal regions analyzed. The boxed region includes the NBNC glial cell referenced in the analysis of polyglutamylated tubulin profiles of the neuronal regions marked by (B). While the polyglutamylated tubulin signal is faint, polyglutamylated tubulin profiles were found to be the most prominent at neuronal regions proximal to contacting and NBNC glial cells.

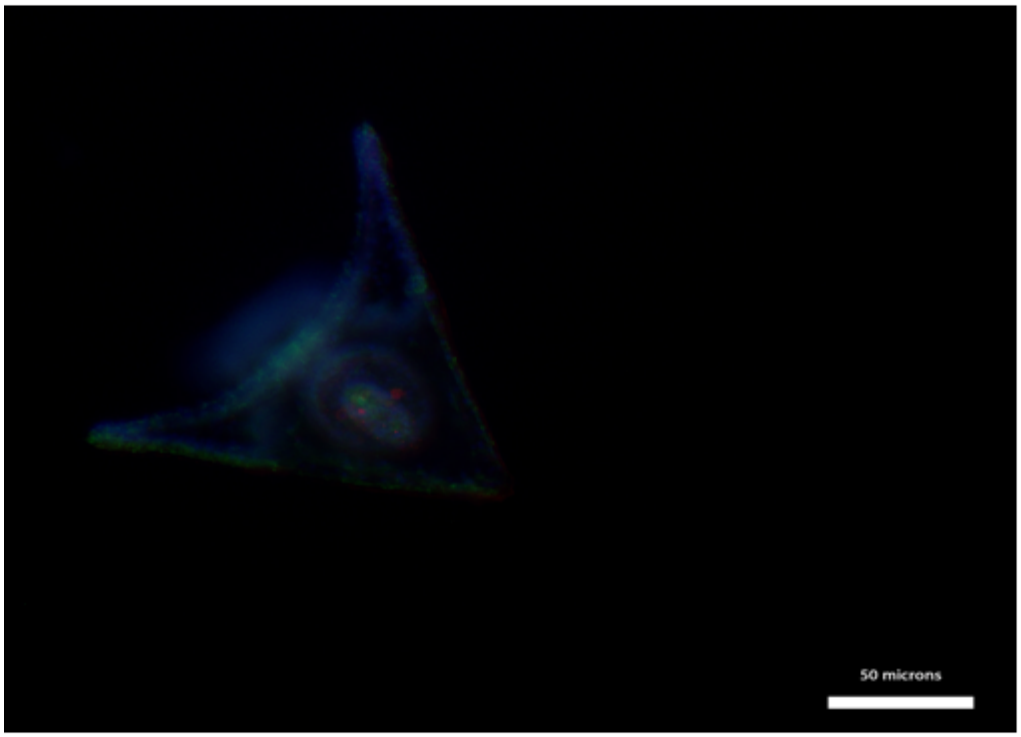

Fig. 2. *L. pictus* plutei larvae fixed with formaldehyde/glutaraldehyde, and stained with Hoechst (blue; DNA), FITC-DM1A (green; α-tubulin), and anti-polyglutamylated tubulin (red; polyglutamylated tubulin), and imaged at 40X objective magnification with a Nikon Eclipse E801 Epi-Fluorescence Microscope. Notice that there are fluorescent signals present in each channel.

It is important to note that different fixatives were used in the preparation of the experimental and positive control samples depicted in Figures 1 and 2 above. While all of the *L. pictus* samples used as the positive controls were fixed with formaldehyde-glutaraldehyde, the methanol-fixed experimental sample shown in Figure 1 was included in the publication because the image (Fig. 1) represented the sorts of analyses done in the present study better than the images derived from the formaldehyde/glutaraldehyde fixed-experimental samples. Nevertheless, it was assumed that the fluorescence observed in the formaldehyde/glutaraldehyde fixed-positive controls would have also been observed if the positive control samples were fixed with methanol.

Neuronal regions proximal to contacting glial cells have greater polyglutamylated tubulin profiles

The polyglutamylated tubulin profiles of proximal and distal neuronal regions associated with contacting glial cells were 0.401±0.256 and 0.149±0.147 respectively (Fig. 3). That is, the neuronal areas within 5 microns of the edges of contacting glial cells had statistically significantly larger polyglutamylated tubulin to α-tubulin ratios than neuronal areas more than 20 microns away from the edges of the same contacting glial cells (P=0.0009; df=34).

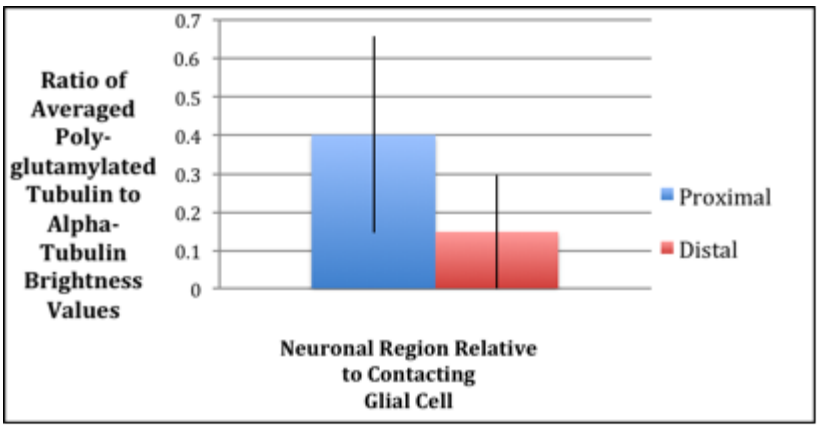

Fig. 3. Polyglutamylated tubulin profile in neuronal regions associated with contacting glial cells. Notice how proximal neuronal regions in contact with glial cells had more tubulin polyglutamylation than distal neuronal regions. Also note the high degree of variability of the pooled ratios (n=18).

Neuronal regions proximal and distal to NBNC glial cells do not have significantly different polyglutamylated tubulin profiles

While neuronal regions proximal and distal to contacting glial cells had significantly different polyglutamylated tubulin profiles, the polyglutamylated tubulin to α-tubulin ratios measured both at neuronal areas within 40 microns and more than 100 microns from the edges of NBNC glial cells were not statistically different (P=0.3979; df=12). The polyglutamylated tubulin profiles of proximal and distal neuronal regions associated with NBNC glial cells were 0.532±0.321 and 0.293±0.646 respectively (Fig. 4).

However, the averaged polyglutamylated tubulin profiles of neuronal regions distal to contacting glial cells and neuronal regions proximal to NBNC glial cells were found to be significantly different (P=0.0004; df=23). Areas distal to contacting glial cells and areas proximal to NBNC glial cells had polyglutamylated tubulin to α-tubulin ratios of 0.532±0.321 and 0.149±0.147 respectively. Despite the high degree of variability in the pooled ratios (n=25), the polyglutamylated tubulin profile of neuronal areas proximal to NBNC glial cells was more than double than that of neuronal areas distal to contacting glial cells.

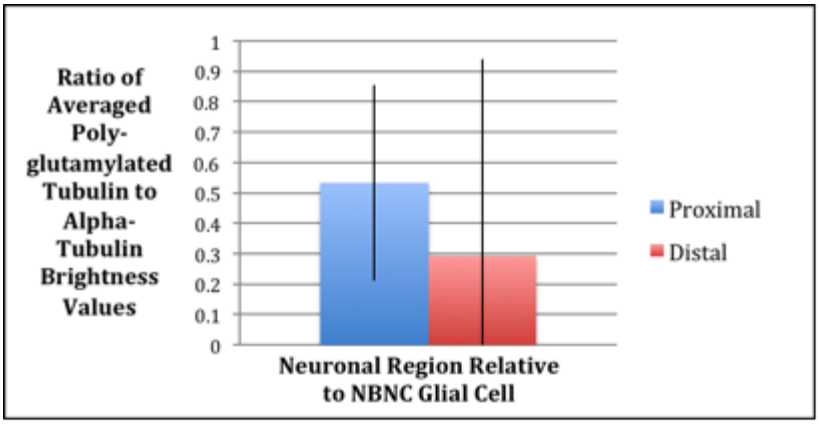

Fig. 4. Polyglutamylated tubulin profile in neuronal regions associated with NBNC glial cells. Contrary to the hypothesized outcome, the polyglutamylated tubulin profiles were not greater in neuronal regions proximal to NBNC glial cells. Note the high degree of variability characteristic of the pooled ratios (n=7).

Discussion

The polyglutamylated tubulin profile data supported the present hypothesis that glial cells influence tubulin glutamylation patterns in neurons. While polyglutamylated tubulin profiles differed significantly between proximal and distal regions of neurons in direct contact with glial cells (Fig. 3), there was no statistically significant difference between polyglutamylated tubulin profiles between proximal and distal regions of neurons neighboring (but not directly in contact with) glial cells (Fig. 4). While no conclusions could be drawn about the molecular mechanisms connecting glial cell signaling to tubulin glutamylation patterns in neurons, the results suggested that neuronal polyglutamylation tubulin profiles correlate with glial cell proximity. Interestingly, the areas on neurons within 40 microns of NBNC glial cells had significantly greater polyglutamylated tubulin profiles than neuronal regions more than 20 microns from contacting glial cells. This finding suggested that the putative effect of directly innervating glial cells on neuronal tubulin glutamylation decreases as a function of distance from the glial cell contact point, and that NBNC glial cells may in fact have a localized effect on neuronal tubulin glutamylation patterns.

The results suggested that glial cells have a role in regulating neuronal tubulin polyglutamylation. This supposition may be reasonable when considering the complex NGF signaling pathway. Once secreted by glial cells, NGF binds to discrete tropomyosin receptor kinases (Trks) on the surface of nearby neurons and triggers a signal transduction cascade that results in both the inhibition of neuronal apoptotic pathways and promotion of cell survival (Kandel et al. 2000). Recent studies also suggest a molecular link between glial cell trophic factor release and microtubule dynamics through mitogen-activated protein kinase (MAPK) signaling pathways mediating NGF's neuroprotective effects via Trk receptors (Nguyen et al. 2009). One relevant reaction that MAPKs catalyze is the phosphorylation of certain MAPs, such as MAP2 and Tau, which has been shown to occur more significantly during neurite outgrowth than in neurite maturation (Sanchez et al. 2000; Sonia et al. 2012). Once phosphorylated, MAPs detach from their tubulin-binding sites and have a destabilizing effect on microtubules that promotes the tubulin

polymerization underpinning neurite outgrowth (Sonia et al. 2012).

It is possible that NGF triggers an additional signaling pathway that leads to the activation of polyglutamylase enzymes to produce the tubulin polyglutamylation patterns potentially necessary for efficient MAP-tubulin binding in the first place. It is not so unlikely that NGF binding could result in a twofold response affecting microtubule dynamics: an increase in polyglutamylation to enhance MAP-tubulin binding, and the phosphorylation of MAPs to alter microtubule stability (Sanchez et al. 2000; Sonia et al. 2012).

However, several methodological approaches could have contributed to the high degree of variability observed in neuronal polyglutamylated tubulin profiles. A total of 25 comparable neuronal regions from 5 imaged slides were analyzed in this study. Such a small sample size could have yielded variable data. Reproductions of this experiment should analyze more chick embryonic nervous system tissue culture samples and corresponding neuron-glial interactions to reduce the variability in poly-glutamylated tubulin profiles seen in this study. It is also important to note that the distances defining proximal and distal areas on neurons relative to both contacting and NBNC glial cells were arbitrarily chosen. Most importantly, the polyglutamylated tubulin signal brightness values recorded could have been inaccurate due to the fluorescent flare radiating from the polyglutamylated tubulin signals from the glial cells themselves. If this were the case, then the calculated polyglutamylated tubulin profiles would not have been accurate quantifications of the tubulin glutamylation patterns in neurons. In future experiments, neuronal polyglutamylated tubulin profiles should be measured incrementally from the glial cell contact point in a gradient sort of approach to establish modified distance parameters (i.e., distances constituting proximal and distal) and discern any effect of fluorescent flare. Lastly, multiple positive controls should also be prepared using all of the fixatives used in the experimental samples (i.e., positive controls should be prepared using both formaldehyde/glutaraldehyde and methanol fixatives).

This experiment served as a pilot study for future investigations of glial cell signaling and its effects on neuronal tubulin glutamylation patterns. The role of glial cells in regulating tubulin polyglutamylation in neurons may be of medical significance, as there is evidence linking neuronal tubulin glutamylation to the molecular workings underlying neurodegeneration associated with physical trauma and Alzheimer's disease (O'Hagan and Barr 2012; Harris et al. 2000; Chen et al. 2011; Ikegami et al. 2006). However, molecular biology techniques should be employed to gain a deeper understanding of the molecular pathways linking glial cell trophic factor signaling to neuronal microtubule polyglutamylation. One potential approach could be to analyze the expression of polyglutamylase-encoding genes as a function of NGF concentration in the nervous system tissue culture medium using quantitative reverse transcription PCR (RT-qPCR) to measure the polyglutamylase mRNA transcript levels. In essence, future steps should aim to pinpoint the effect of NGF or other glial-cell secreted trophic factors on neuron-expressed polyglutamylase function.

References

Audebert, S., A. Koulakoff, Y. Berwald-Netter, F. Gros, P. Denoulet, and B. Edde. 1994. Developmental regulation of polyglutamylated alpha- and beta-tubulin in mouse brain neurons. *Journal of Cell Science* 107: 2313-2322.

Chen, Lizhen, Z. Wang, A. Ghosh-Roy, T. Hubert, D. Yan, S. O'Rourke, B. Bowerman, Z. Wu, Y. Jin, and A.D. Chrisholm. 2011. Axon regeneration pathways identified by systemic genetic screening in *C. elegans*. *Neuron* 71(6): 1043-1057.

Harris, A., J.I. Morgan, M. Pecot, A. Soumare, A. Osborne, and H.D. Soares. 2000. Regenerating motor neurons express Nna1, a novel ATP/GTP-binding protein related to zinc carboxypeptidases. *Molecular and Cellular Neuroscience* 16(5): 578-596.

Ikegami, K., M. Mukai, J. Tsuchida, R.L. Heier, G.R. Macgregor, and M. Setou. 2006. TTLL7 is a mammalian β-tubulin polyglutamylase required for growth of MAP2-positive neurites. *Journal of Biological Chemistry* 281: 30707-30716.

Kandel, Eric R., James H. Schwartz, Thomas M. Jessell, Steven A. Siegelbaum, and A.J. Hudspeth. 2000. *Principles of Neural Science*. 5th ed. New York: McGraw-Hill, Health Professions Division.

Morris, R. L., and P.J. Hollenbeck. 1993. The regulation of bidirectional mitochondrial transport is coordinated with axonal outgrowth. *Journal of Cell Science* 104: 917-927.

Morris, R.L. 2013. Immunofluor staining of SU embryos – MeOH fixation. *Bio324/Neurobiology, Wheaton College*.

Morris, R.L. 2014. Immunofluorescence of chick neuronal primary cultures. *Bio324/Neurobiology, Wheaton College*.

Morris, R.L. 2014. Primary culture of chick embryonic peripheral neurons1: dissection. *Bio324/Neurobiology, Wheaton College*.

Nguyen, N., S.B. Lee, Y.S. Lee, K.H. Lee, and J.Y. Ahn. 2009. Neuroprotection by NGF and BDNF against neurotoxin-

exerted apoptotic death in neural stem cells are mediated through Trk receptors, activating PI3-kinase and MAPK pathways. *Neurochemical Research* 34: 942-951.

O'Hagan, Robert and Maureen M. Barr. 2012. Regulation of tubulin glutamylation plays cell-specific roles in the function and stability of sensory cilia. *Worm* 1(3): 155-159.

Sakakibara, A., R. Ando, T. Sapir, and T. Tanaka. 2013. Microtubule dynamics in neuronal morphogenesis. *Open Biology* 3(7).

Sanchez, C., J. Diaz-Nido, and J. Avila. 2000. Phosphorylation of microtubule-associated protein 2 (MAP2) and its relevance for the regulation of the neuronal cytoskeletal function. *Progressive Neurobiology* 62(2): 133-168.

Sonia, A., L. Correa, and K.L. Eales. 2012. The role of p38 MAPK and its substrates in neuronal plasticity and neurodegenerative disease. *Journal of Signal Transduction* 2012.

Wloga, Dorota and Jacek Gaertig. 2011. Post-translational modifications of microtubules. *Journal of Cell Science* 124(1): 154.